Adsorption Science & Technology

15th Ukrainian-Polish Symposium

Adsorption Science & Technology
2017, Vol. 35(5–6) 507–518

DOI: 10.1177/0263617417698966
journals.sagepub.com/home/adt
SAGE

The influence of the hydroxyapatite synthesis method on the electrochemical, surface and adsorption properties of hydroxyapatite

Ewa Skwarek, Władysław Janusz and Dariusz Sternik
Faculty of Chemistry, Maria Curie-Skłodowska University, Poland

Abstract
Hydroxyapatite is a compound that belongs to the group of apatite minerals. It is a very interesting adsorbent and the main inorganic component of bones and teeth. Hydroxyapatite was obtained using three different methods. The samples were designated as HAP1, HAP2 and HAP3. The synthesized adsorbents were characterized by the following methods: thermal analysis, EDAX, XRD, FTIR, adsorption and desorption of nitrogen. The electrochemical properties were studied by electrochemical titration and zeta potential. The protein used was bovine serum albumin; its concentration was 5 mg/ml. The adsorbed protein concentration was determined based on the absorbance measurements at $\lambda = 279$ nm by UV-VIS. The characteristics are pHpzc = 6.64, 6.22, 6.43 at the HAP1/NaCl, HAP2/NaCl, HAP3/NaCl interfaces respectively and the pHiep values are about 4 for all the systems. The thermal stability of hydroxyapatite changed due to the bovine serum albumin adsorption. Synthesis method of hydroxyapatite influences on electrochemical properties and adsorption of bovine serum albumin on it.

Keywords
Hydroxyapatite, BSA (bovine serum albumin), adsorption, EDL (electrical double layer), thermal analysis

Submission date: 19 December 2016; Acceptance date: 1 February 2017

Corresponding author:
Ewa Skwarek, Faculty of Chemistry, Maria Curie-Skłodowska University, pl. Maria Curie-Skłodowskiej 3, 20-031 Lublin, Poland.
Email: ewunias@hektor.umcs.lublin.pl

Introduction

Hydroxyapatite is the main component of tooth enamel, dentine and vertebrate bones. In living organisms, it undergoes continuous dissolution, recrystallization and hydrolytic processes. Hydroxyapatites are used in orthopaedics, stomatology, laryngology and cosmetics. The interest in the modification of hydroxyapatite with proteins results from the fact that these bio components are simple, very well characterized chemical compounds which facilitate physicochemical studies and thereby their application. Adsorption is one of the ways used for the modification of the hydroxyapatite surface structure. Before protein adsorption, pure hydroxyapatite is prepared according to one of the synthesis methods described in literature. The positions above describes the proteins adsorption on different adsorbents (Rose et al., 2002; Skwarek et al., 2014; Szewczuk–Karpisz et al., 2014, 2015; Wisniewska et al., 2015). The other method of the adsorption procedure is done by placing the hydroxyapatite in an aqueous solution of protein. The obtained suspension is mixed or shaken for a fixed time, then it is centrifuged (or filtered), and finally the deposit is dried. In such an adsorption process, a large number of parameters should be taken into account and their values should be adjusted during the adsorption optimization (Janusz et al., 2014). The most important parameter is the molar ratio Ca/P of the initial hydroxyapatite, the value 1.67 is characteristic of stoichiometric hydroxyapatite [$Ca_{10}(PO_4)_6(OH)_2$], commonly used as an adsorbent. It was found that with the decreasing molar ratio Ca/P, the tendency to amino acid adsorption increases similar to that of proteins. Decrease in this ratio (Ca/P) is usually caused by a drop in calcium ion content compared to that of phosphorus, which preserves the neutral electrical charge of the whole crystal lattice owing to the ion substitution. It was also proved that adsorption effectiveness increases with the increasing amount of HPO_4^{2-} ions in the hydroxyapatite crystal in the places originally occupied by PO_4^{3-} ions. Substitution of tri-negative ion by the di-negative one results in changes in the crystal structure leading to charge compensation by local losses and/or incorporation of other ions. The smallest value of the ratio Ca/P in non-stoichiometric hydroxyapatite used for amino acid adsorption was 1.33 and its formula is: $Ca_8(PO_4)_{3.5}(HPO_4)_{2.5}(OH)_{0.5}$.This formula has a proper zero total charge and indicates a large content of HPO_4^{2-} ions necessary for the effective adsorption of amino acids (Rhilassi et al., 2012). The effect of the hydroxyapatite mass and protein solution volume as well as protein concentration in the solution on adsorption effectiveness is obvious. These parameters should be selected depending on the known specific surface area of hydroxyapatites on which adsorption proceeded so that the amount of protein should correspond to the saturation of the surface of crystals suspended in the solution. Protein interactions with the hydroxyapatite structure depend on the kind and ionization of the protein itself. In turn, ionization degree depends on the pH of the solutions. There are many factors that affect the adsorption which creates problems connected with elaboration of modification conditions. Therefore, many adsorption parameters are chosen in an empirical way using the trial and error method. A typical example is adjustment of temperature maintained during the contact time of hydroxyapatite with the protein solution. On the molecular level, adsorption of any protein on the hydroxyapatite surface is largely dependent on the kind of its ionization as electrostatic interactions are the basic kind of hydroxyapatite–protein interactions. Considering this problem, two types of such interactions can be distinguished: between calcium Ca^{2+} ions of hydroxyapatite and ionized carboxylic –COO– groups of proteins, between phosphate PO_4^{3-}, HPO_4^{2-} groups of hydroxyapatite and ionized amine NH^{3+} groups of proteins (Koutsopoulos et al., 2000;

Sharma et al., 2012). It is also possible that hydrogen bonds are formed between the amine groups of proteins and phosphate groups of hydroxyapatite (Zhou et al., 2007). Van der Waals interactions should be also taken into account. In this paper, we describe the electrical double layer (EDL) at the hydroxyapatite/protein/electrolyte solution interface on the basis of the potentiometric titration of suspension and electrokinetic measurements. These measurements were complemented by the thermogravimetric and FTIR studies of the hydroxyapatite/protein samples. This can be applied for the chromatographic separation of proteins and transportation of drugs on hydroxyapatite in the presence of proteins.

Experimental methods

Synthesis of hydroxyapatites

The investigated adsorbents were synthesized using three methods (Liu et al., 2003; Suzuki et al., 1998; Dean-Mo et al., 1995). Moreover, hydroxyapatite was prepared using three methods:

Method 1: (HAP1) (Liu et al., 2003). Synthetic hydroxyapatite was prepared hydrothermally according to the reaction

$$6CaHPO_4 \cdot 2H_2O + 4Ca(OH)_2 \rightarrow Ca_{10}(PO_4)_6(OH)_2 + 18H_2O$$

In order to prepare the hydroxyapatite, the following procedure was applied: 1.03 g of $CaHPO_4 \times 2\ H_2O$ from Fluka and 0.3 g of $Ca(OH)_2$ from Aldrich were taken and mixed. Eighty millilitres of doubly distilled water were poured in and the pH value was reduced to 9 using 80% of analytically pure acetic acid from POCh. The reaction mixture was put into a drier for 24 hours at 120°C. The obtained hydroxyapatite had to be purified from reagents so the sediment was washed many times with redistilled water and centrifuged.

Method 2: (HAP2) (Suzuki et al., 1998). In this method, the following reagents were used: calcium acetate $(CH_3COO)_2Ca$ from Fluka and dipotassium hydrophosphate K_2HPO_4 from POCh, Gliwice. The solutions of the concentrations 0.1 M K_2HPO_4 and 0.06 M – $(CH_3COO)_2Ca$ were prepared. In the reaction, 0.15 dm^3 of each salt was taken and both solutions were dropped into 0.2 dm^3 of water placed in the reaction flask. The flask was immersed in a water bath and heated up to 100°C. The salt solutions were dropped in at the same time for 30 minutes and then the reaction mixture was boiled for 1 hour. The mixture was stirred vigorously and the constant temperature was maintained all the time. The obtained sediment was washed with redistilled water till the constant value of redistilled water conductivity was achieved.

Method 3: (HAP3) (Dean-Mo et al., 1995). In this method, the following reagents were used:

$$10Ca(OH)_2 + 6H_3PO_4 \rightarrow Ca_{10}(PO_4)_6(OH)_2 + 18H_2O$$

Calcium hydroxide $Ca(OH)_2$ was procured from Aldrich and phosphoric acid, H_3PO_4 (V), from POCh Gliwice. These were mixed to form 1 M aqueous solutions with the reagents; 0.3 $dm^3$of phosphoric acid and 0.18 dm^3 of calcium base were used in the reaction. The H_3PO_4 solution was dropped into the $Ca(OH)_2$ suspension placed in the flask

for 15 minutes. While dropping, the reaction mixture was stirred vigorously and then dried in a dryer for 24 hours. A white sediment of the crystalline structure of hydroxyapatite was obtained. Then, the sediment was washed with redistilled water till the constant value of redistilled water conductivity was achieved.

Adsorption proteins on hydroxyapatite

The protein used was: Bovine serum albumin (BSA)—Sigma Aldrich, and its concentration was 5 mg/ml. Active hydroxyapatite was dried at 100°C for 5 hours. Albumin (BSA) on NaCl solution and hydroxyapatite (0.5 g) were poured to the plastic reactors. The suspensions were mixed at 25°C with 120 r/min for 24 hours. Then the adsorbent was separated from the solution, dried at room temperature in desiccators with molecular sieves for three days and heated at 45°C for 24 hours. The suspension was centrifuged and the adsorbed protein concentration was determined by the difference in absorbance before and after modification at $\lambda = 279$ nm by UV-VIS.

Methods characterizing the surface

Ca and P amounts in hydroxyapatite were determined using the EDX method. Hydroxyapatite was investigated using X-ray diffraction (XRD). A crystallographic structure of samples was determined by XRD using the DRON-3 diffractometer using CuK_α radiation, adsorption–desorption of nitrogen (ASAP2405-Accelerated Surface Area and Porosimetry, Micromeritics Instruments, Co.). Surface charge measurements were performed simultaneously in the suspension of the same solid content, to keep the identical conditions of the experiments in a thermostated Teflon vessel at 25°C. To eliminate the influence of CO_2, all potentiometric measurements were performed under nitrogen atmosphere. pH values were measured using a set of glass REF 451 and calomel pHG201-8 electrodes with the Radiometer assembly. Surface charge density was calculated from the difference of the amounts of added acid or base to obtain the same pH value of suspension as for the background electrolyte. The zeta potential and particle size as well as distribution of hydroxyapatite dispersions were determined by electrophoresis with Zetasizer 3000 by Malvern. The κa was greater than 100, so to calculate the zeta potential, the Smoluchowski's equation was used. The measurements were performed at 100 ppm solid of concentration ultrasonication of the suspension. Thermal analysis was carried out on an STA 449 Jupiter F1, Netzsch (Germany) under the following operational conditions: heating rate of 10°C min^{-1}, dynamic atmosphere of synthetic air (40 ml min^{-1}), temperature range of 30–950°C, sample mass ~16 mg, sensor thermocouple type S TG-DTA. As a reference, empty platinum crucible was used. Pure hydroxyapatite and that after protein adsorption were measured spectroscopically using FTIR Nicolet 8700A apparatus manufactured by Thermo Scientific.

Results and discussion

The Ca:P molar ratios for HAP1, HAP2 and HAP3 are found to be 1.66, 1.65 and 1.64, respectively. These properties are the results of the decreasing amount of calcium ions in the sample determined using the EDAX method that is as follows: 28.2 atom% for HAP1, 21.9 atom% for HAP2 and 22.8 atom% for HAP3. pHpzc of the studied compound is 6.64 for

HAP1, 6.22 for HAP2, 6.43 for HAP3 which is in agreement with the literature data (Rose et al., 2002; Janusz et al., 2008; Skwarek, 2014). The pHpzc values of these samples can be correlated with the calcium content in the hydroxyapatite surface, if the surface hydroxyapatite contains more calcium, then pHpzc is higher. EDL consists of condensed and diffused parts. The value which can be experimentally determined for the condensed layer is pHpzc. This can be done by the potentiometric titration whereas the diffusion layer is characterized by the zeta potential and pHiep. The point of zero charge (pHpzc) corresponds to the zero condition at the surface. The surface of hydroxyapatite can be contaminated with acidic groups when pHpzc is higher than 6. The process of hydroxyapatite synthesis might be its source. The course of dependence of ζ potential shows that the zeta potential decreases with the increasing pH value for all the hydroxyapatite samples (Figures 1 to 3). Extrapolation of the dependence of zeta potential in the pH function lets us assume that pH_{IEP} is about 4 for HAP3 so it is over 2 pH units lower than pH_{PZC} for HAP2 and 1 is HAP3 so it is also lower than pHpzc of the examined samples because the zeta potential is additionally dependent on the part of surface load which is connected with adsorption and desorption of ions of the crystal lattice, that is phosphate and calcium ions. On the XRD spectrum of the samples, one can observe peaks characteristic of crystal form of hydroxyapatite, i.e. peaks and their intensities occurring at the angles: 2θ: 25.9–35%; 31.75–100%; 32.96–55%; 39.84–20%; 46.7–40%; 49.5–30%. The size of crystallites

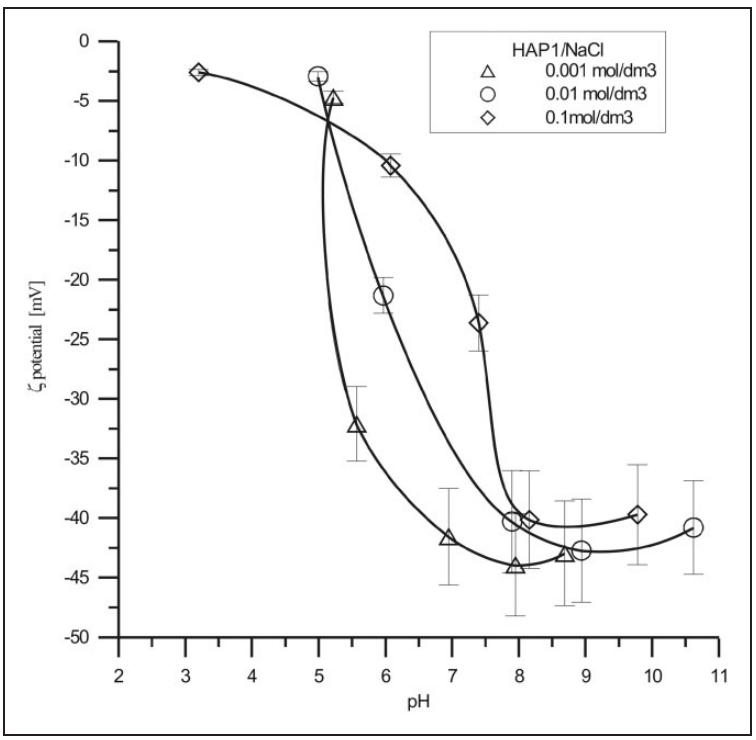

Figure 1. Zeta potential of the HAP1/NaCl solution interface as a function of pH.

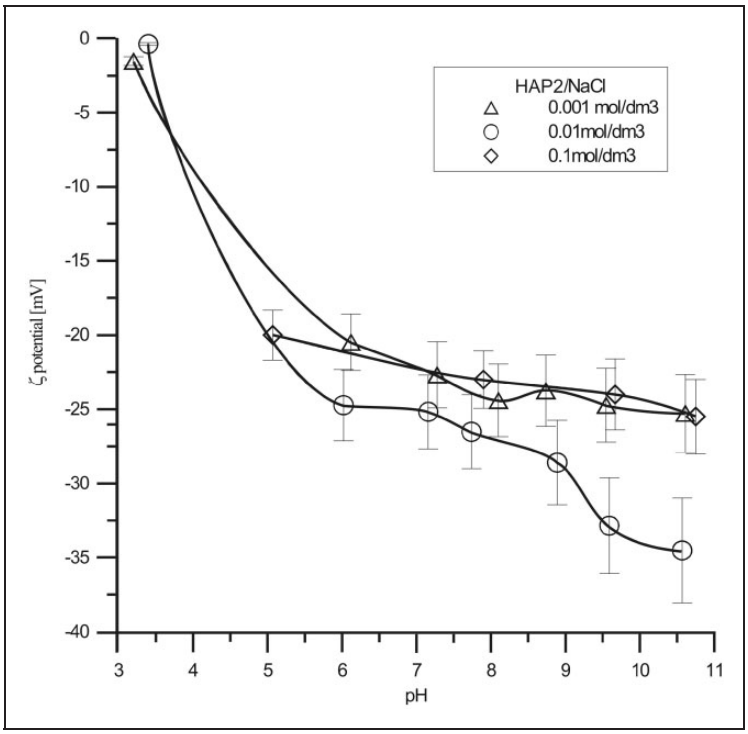

Figure 2. Zeta potential of the HAP2/NaCl solution interface as a function of pH.

calculated with the Scherer's method from half width of the peak for the angle $2\Theta = 25.9$ was 44 nm for HAP1, 34 nm for HAP2 and 23 nm for HAP3. These results agree well with the abovementioned surface area measurements. The results of the XRD studies can contribute to understanding the adsorption of BSA protein on hydroxyapatite (Zhuang et al., 2013). Adsorption of negatively charged BSA proteins can proceed on various crystalline planes of hydroxyapatites prepared by various methods. The results indicate that the a-plane of HAP crystals is selective for the adsorption of acidic proteins such as BSA. The a-planes of HAP crystals are rich in positively charged calcium ions; therefore, acidic negatively charged proteins are more readily adsorbed by the electrostatic force of attraction which is also confirmed by thermal studies. Diffractometric studies of hydroxyapatite materials modified with proteins enables first of all analysis of the effect of these proteins on the mineral crystal lattice (crystalline elementary cell parameters). It was found out that the effect of protein adsorption does not change the sample crystallinity itself. Based on the results using the Photon Correlation Spectroscopy (PCS) method, it can be stated that all samples are polydispersive. The particle diameter ranges from 2 μm to 300 μm, one can see that in all cases, as a result of the synthesis, aggregations of hydroxyapatite molecules are obtained. From the sizes of crystallites determined on the basis of XRD method it can be concluded that hydroxyapatite particle consists of a huge number of crystals which lead to porous structure formation. The BSA protein has been chosen for measurements due to its $pHiep = 5.82$ and is similar to pHpzc obtained hydroxyapatites. At the hydroxyapatite/electrolyte solution interface phases a form of matter during separation proteins mixture by

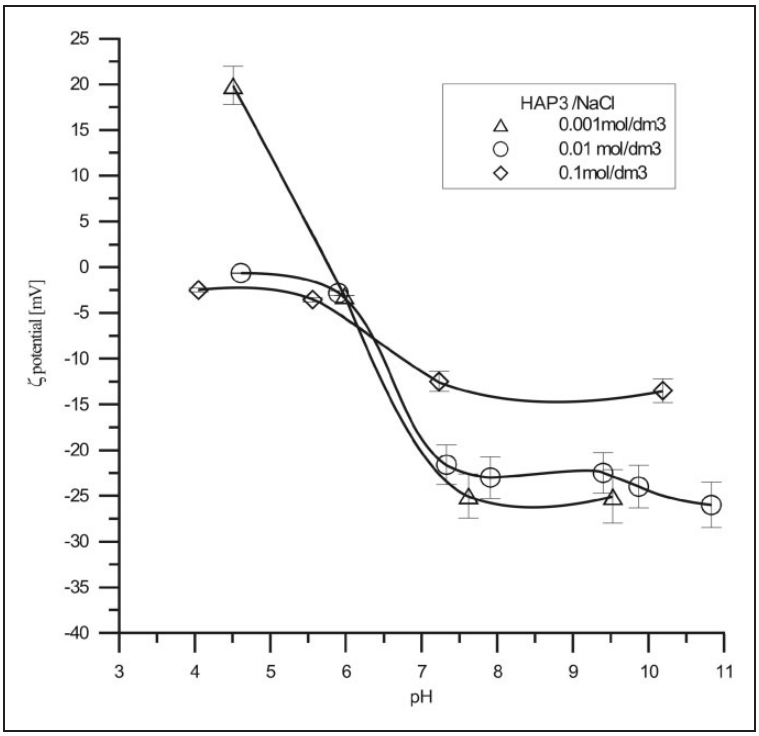

Figure 3. Zeta potential of the HAP3/NaCl solution interface as a function of pH.

electrophoresis. The adsorption phenomenon of BSA on hydroxyapatite is attributed to the electrostatic interactions between Ca^{2+} cation and PO_4^{3-} anion of hydroxyapatite with COO− anion and NH^{4+} cation of BSA protein, respectively.

Table 1 presents the structural parameters of hydroxyapatite. On the basis of the results in Table 1, the difference in the surface area and average volume of pores can be seen. The surface area and average volume of pores of sample 3 are larger than those of samples 2 and 1. The analyzed samples of hydroxyapatite have mesopores, a significant difference in the size of the surface itself, which confirms the influence of the synthesis method, can be also observed. Protein on the hydroxyapatite surface can adsorb or build into its structure decreasing the specific surface area of the samples and increasing pores on the surface. Protein gets into the hydroxyapatite pores.

Figure 4 presents the TG and DTG curves of thermal distributions of hydroxyapatites obtained using various methods. In the case of hydroxyapatites, two characteristic ranges of transformations due to heating up to 1000°C can be distinguished. In the temperature range 30–700°C mass losses and peaks on the TG and DTG are associated with removal of physically adsorbed water (Bianco et al., 2007), the hydration layers of HPO_4^{2-} ions (Kazuhiko et al., 2009) as well as with decomposition of carbonates remained after the synthesis (Pang et al., 2003; Rose et al., 2002). At high temperatures above 700°C, the processes are connected with the reaction of $P_2O_7^{4-}$ ions and OH^- ions (Skwarek et al., 2014). The BSA adsorption changes the thermal stability of hydroxyapatites (Figure 5) and the temperatures of individual stages moved to lower ones.

Table 1. Chosen structural parameters, HAP1, HAP2 and HAP3.

	HAP1	HAP1/BSA	HAP2	HAP2/BSA	HAP3	HAP3/BSA
BET surface area [m^2/g]	28	16	47	30	131	76
Langmuir surface area [m^2/g]	37	25	60	46	167	115
BJH cumulative adsorption surface area of pores between 1.7 and 300 nm diameter [cm^3/g]	0.011	1.66	0.024	2.95	0.055	7.63
BJH cumulative desorption surface area of pores between 1.7 and 300 nm diameter [cm^3/g]	0.011	3.05	0.023	3.17	0.056	8.22
Average pore diameter (4V/A by BET) [nm]	13.19	23.46	15.47	19.66	15.88	24.41
BJH adsorption on average pore diameter (4V/A) [nm]	13.05	23.05	17.53	20.26	14.60	24.42
BJH desorption on average pore diameter (4V/A) [nm]	9.23	12.55	16.36	19.00	13.80	22.73

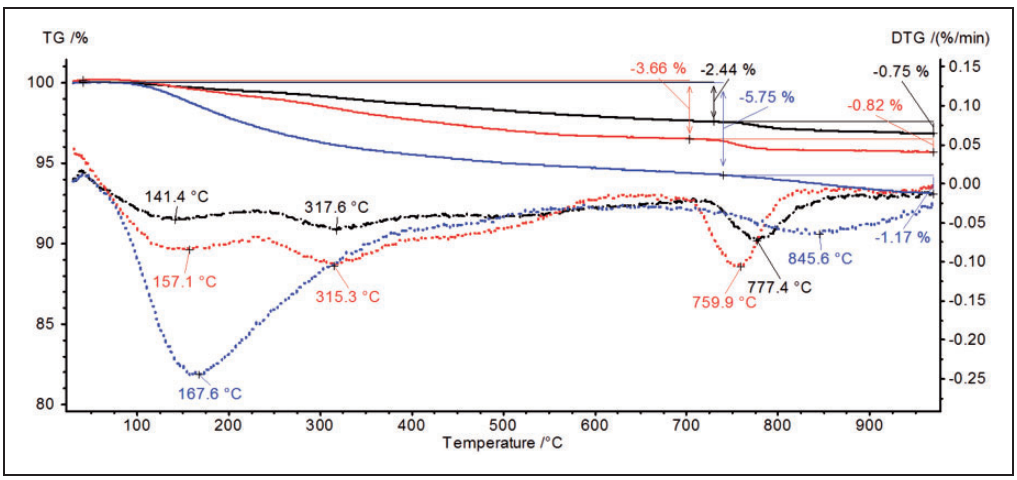

Figure 4. TG (continuous line) and DTG (broken line) curves of hydroxyapatite samples: HAP1 (black colour), HAP2 (red colour) and HAP3 (blue colour).

Mass losses observed for the samples after modification are little larger in relation to initial materials (the biggest for the sample HAP3-BSA ($\Delta m = \sim 7.28\%$)). Due to the modification with protein, two additional peaks in the temperature range 200°C to 500°C appeared on the DTG (red line) and DTA (blue line) curves as a result of exothermic process connected with the decay of BSA molecules (Han et al., 2007; Sanjaya et al., 2013). These peaks in this range are associated with the defragmentation and partial oxidation of BSA molecules. Differences on DSC curves are probably results of existence of two kinds of

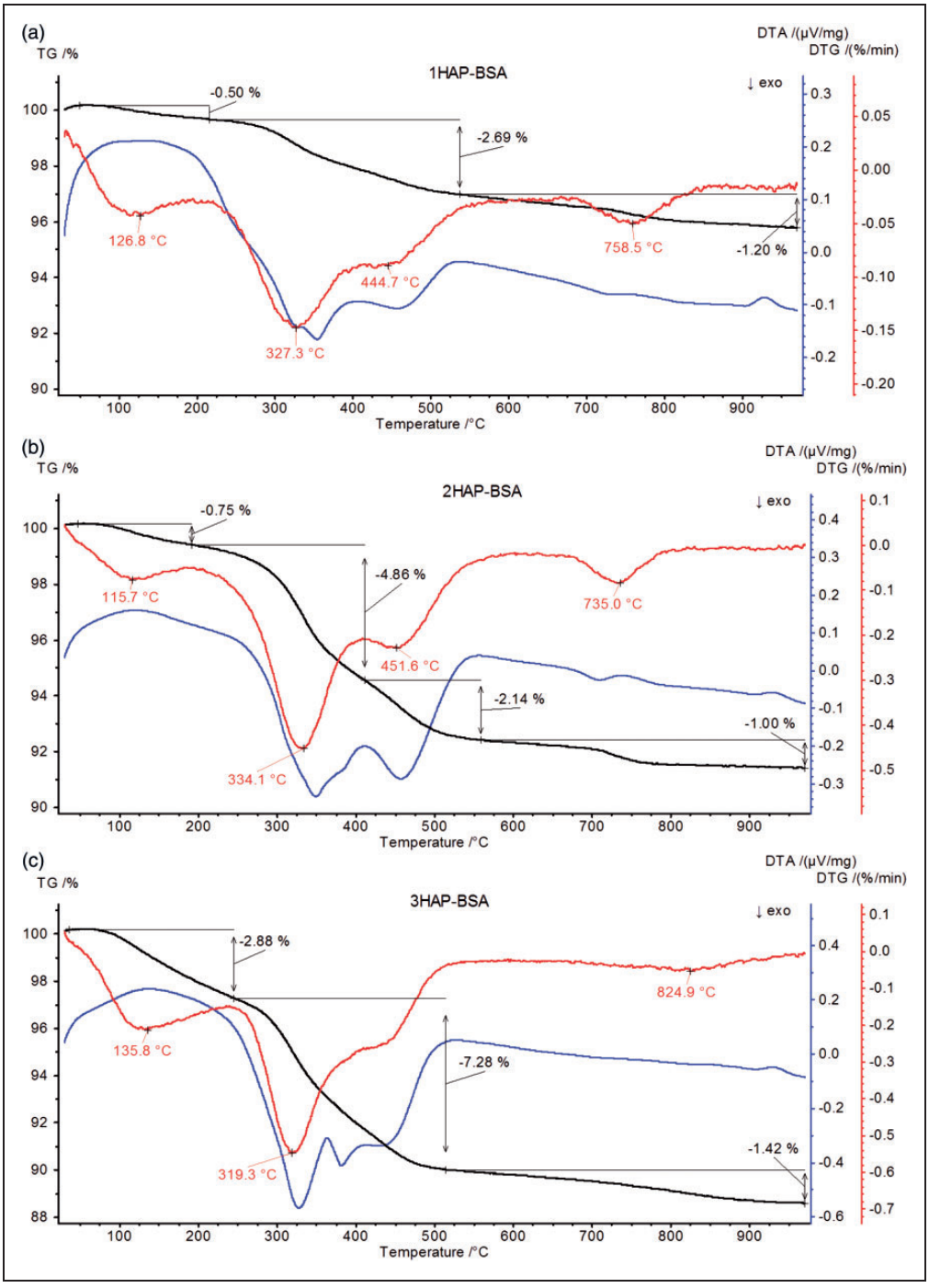

Figure 5. TG (black line), DTG (red line) and DSC (blue line) curves for hydroxyapatite samples modified by BSA.

macromolecules on the surface bound by means of electrostatic interactions and Van der Waals forces, similar to the clays modified with surfactants (Majdan et al., 2010). Due to the fact that adsorbed protein undergoes partial denaturation, its secondary structure is identical to the thermally denatured form (Giacomelli et al., 2001; Norde et al., 2000). The first peak in the temperature range 310–340°C on the DTA curve is associated with the removal of BSA molecules weakly bounded with the adsorbent surface and the second one in the temperature range 400–500°C with the distribution of the molecules strongly bound with the surface (Dasgupta et al., 2010). For all the cases, the same amount of BSA was absorbed at the similar surface. The characteristic electrochemical parameter—point pHiep for BSA equals to 5.82 and is very similar to the pHpzc values for studied hydroxyapatites, so different thermal stability of BSA adsorbed at hydroxyapatite can lead to the conclusion that the synthesis method has an impact. It is interesting to note that higher Ca:P ratio of hydroxyapatites preferentially adhered more amount of COO^{-} group from the protein surface which ultimately enhances the decomposition phenomenon. Similarly, low Ca:P ratio of HAP promotes a relatively intense adhesion through more anionic PO_4^{3-} group and NH^{4+} of protein, which finally needs more temperature to remove BSA. Thus, the thermal analysis of BSA adsorbed hydroxyapatite clarifies the adherence of BSA particles to the surface of the hydroxyapatite through the electrostatic force of attraction. The FTIR spectra of the hydroxyapatite samples HAP1, HAP2, HAP3 and samples with protein adsorbed are depicted in Figure 6. It shows the characteristic bands of PO_4 at the wave numbers: 565, 603, 962–1033 cm^{-1}, the presence bands of CO_3 at the wavenumbers

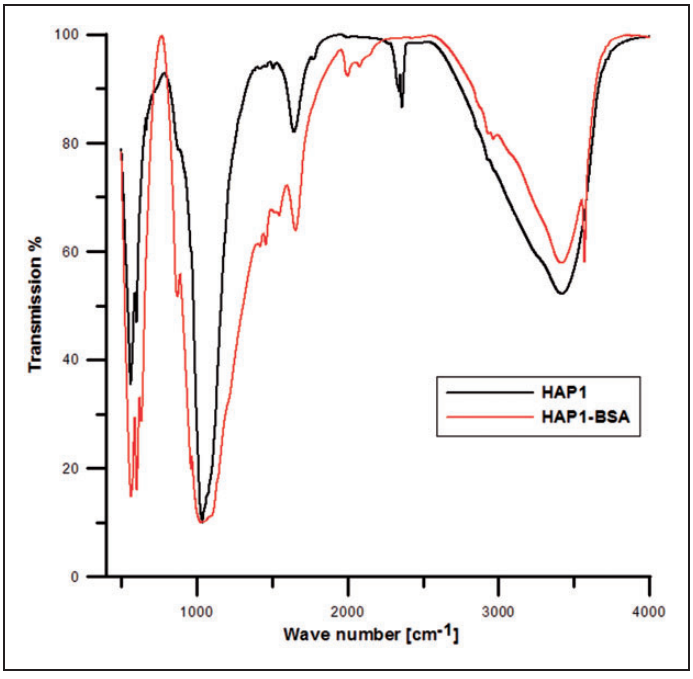

Figure 6. Transmission spectrum of hydroxyapatite and BSA.

1421–1489 cm^{-1} and the bands of OH groups at 3570 cm^{-1}. The peak near 1650 cm^{-1} in Figure 6 is the amide I band. It results from the C=O stretching vibrations of the peptide bond. Similarly, the peaks near 1540 cm^{-1} (N–H bending vibration/C–N stretching vibration) and 1240 cm^{-1} (C–N stretching vibration/N–H bending vibration) are called amide II band, and amide III band, respectively. The peak near 3300 cm^{-1} is thought to be N–H bending vibration. The peak near 1400 cm^{-1} result from protein side-chain COO–. Carbonate and water (OH group) in hydroxyapatite is believed to affect the protein adsorption.

Conclusions

Hydroxyapatite synthesized by three different methods exhibits different surface composition and properties. The results of X-ray diffraction analysis and that of specific surface area obtained by BET indicate the relationship between the synthesis and structure parameters. The hydroxyapatite synthesized differently had different particle size distribution. The synthesis method of hydroxyapatite influences greatly on its electrochemical properties – zeta potential, pHpzc and pHiep and colloidal stability. Characteristics of the EDL at the HAP1/NaCl interface pHpzc = 6.64, for the HAP2/NaCl interface pHpzc = 6.22, for HAP3/NaCl interface pHpzc = 6.43, the pHiep values for all the systems are about 4. Due to adsorption of BSA, thermal stability of hydroxyapatites changed and the temperature of individual stages moved to lower temperatures. FT-IR spectra of samples give information about carbonate and water (OH group) in samples as well as P–O bonding. Carbonate and water (OH group) in hydroxyapatite are believed to affect the protein adsorption. The results of this study indicate that the method of synthesis of HAP has an influence on its electrochemical, surface and adsorption properties.

Declaration of Conflicting Interests

The author(s) declared no potential conflicts of interest with respect to the research, authorship, and/or publication of this article.

Funding

The author(s) disclosed receipt of the following financial support for the research, authorship, and/or publication of this article: This research was funded by the People Programme (Marie Curie Actions) of the European Union's Seventh Framework Programme FP7/2007-2013/ under REA grant agreement no. PIRSES-GA-2013-612484.

References

Bianco A, Cacciotti I, Lombardi M, et al. (2007) Thermal stability and sintering behavior of hydroxyapatite nanopowders. *Journal of Thermal Analysis and Calorimetry* 88(1): 237–243.

Dasgupta S, Bandyopadhyay A and Bose S (2010) Zn and Mg doped hydroxyapatite nanoparticles for controlled release of protein. *Langmuir* 26(7): 4958–4964.

Dean-Mo L (1996) Fabrication and characterization of porous hydroxyapatite granules. *Biomaterials* 17: 1955–1957.

Giacomelli CE and Norde W (2001) The adsorption–desorption cycle. Reversibility of the BSA-silica system. *Journal of Colloid and Interface Science* 233: 234–240.

Han Y, Li S, Wang X, et al. (2007) Preparation of hydroxyapatite rod-like crystals by protein precursor method. *Materials Research Bulletin* 42(6): 1169–1177.

Janusz W, Gałgan A and Skwarek E (2004) Effects of the adsorption of Ba^{2+} ions on the electrical double layer at the 4th group metal oxide/electrolyte interface. *Adsorption Science Technology* 22(10): 795–805.

Janusz W, Skwarek E, Złotucha A, et al. (2008) The electrical double layer at the hydroxyapatite/$NaClO_4$ solution interface. *Polish Journal Chemistry* 82(1–2): 57–69.

Koutsopoulos S and Dalas E (2000) The effect of acidic amino acids on hydroxyapatite crystallization. *Journal of Crystal Growth* 217: 410–415.

Kazuhiko K, Mizumoto S, Toshima S, et al. (2009) Effects of heat treatment of calcium hydroxyapatite particles on the protein adsorption behavior. *Journal of Physical Chemistry B* 113: 11016–11022.

Liu J, Ye X, Wang H, et al. (2003) The influence of pH and temperature on the morphology of hydroxyapatite synthesized by hydrothermal method. *Ceramic International* 29: 629–637.

Majdan M, Pikus S, Gajowiak A, et al. (2010) Uranium sorption on bentonite modified by octadecyltrimethyl ammonium bromide. *Journal of Hazardous Materials* 184: 662–670.

Norde W and Giacomelli CE (2000) BSA structural changes during homomolecular exchange between the adsorbed and the dissolved states. *Journal of Biotechnology* 79: 259–268.

Pang YX and Bao X (2003) Influence of temperature, ripening time and calcinations on the morphology and crystallinity of hydroxyapatite nanoparticles. *Journal of the European Ceramic Society* 23: 1697–1704.

Rhilassi AE, Mourabet M, Boujaady HE, et al. (2012) Use of response surface methodology for optimization of fluoride adsorption in an aqueous solution by Brushite. *Applied Surface Science* 259: 376–384.

Rose ME, Huerbin MB, Melick J, et al. (2002) Regulation of interstitial excitatory amino acid concentrations after cortical contusion injury. *Brain Researcher* 935(12): 40–46.

Sanjaya KS and Debasish S (2013) Study of BSA protein adsorption/release on hydroxyapatite nanoparticles. *Applied Surface Science* 286: 99–103.

Sharma R, Pandey RR, Gupta AA, et al. (2012) In situ amino acid functionalization and microstructure formation of hydroxyapatite nanoparticles synthesized at different pH by precipitation route. *Materials Chemistry and Physics* 133: 718–725.

Skwarek E (2014) Adsorption of Zn on synthetic hydroxyapatite from aqueous solution. *Separation Science and Technology* 49(11): 1654–1662.

Skwarek E, Janusz W and Sternik D (2014) Adsorption of Citrate Ions on Hydroxyapatite Synthesized by various methods. *Journal of Radioanalytical and Nuclear Chemistry* 299(3): 2027–2036.

Suzuki S, Ohgaki M, Ichiyanagi M, et al. (1998) Preparation of needle-like hydroxyapatite. *Journal of Material Science Letters* 17: 381–395.

Szewczuk-Karpisz K and Wiśniewska M (2014) Adsorption properties of the albumin-chromium (III) oxide system – Effect of solution pH and ionic strength. *Soft Materials* 12(3): 268–276.

Szewczuk-Karpisz K and Wiśniewska M (2015) Investigation of removal possibilities of chromium (III) oxide from water solution in the presence of albumins. *International Journal of Environmental Science and Technology* 12: 2947–2956.

Wïniewska M, Szewczuk-Karpisz K and Sternik D (2015) Adsorption and thermal properties of the bovine serum albumin-silicon dioxide system. *Journal of Thermal Analysis and Calorimetry* 120: 1355–1364.

Zhou H, Wu T, Dong X, et al. (2007) Adsorption mechanism of BMP-7 on hydroxyapatite (001) surfaces. *Biochemical and Biophysical Research Communications* 361: 91–96.

Zhuang Z and Aizawa M (2013) Protein adsorption on single-crystal hydroxyapatite particles with preferred orientation to a(b)- and c-axes. *Journal of Material Science: Material Medicine* 24: 1211–1216.